Aalto University Publications in Materials Science and Engineering
Aalto-yliopiston materiaalitekniikan julkaisuja
Espoo 2010 TKK-MT-215

Densities of Molten and Solid Alloys of (Fe, Cu, Ni, Co) - S at Elevated Temperatures - Literature Review and Analysis

F. Tesfaye Firdu, P. Taskinen

Aalto-yliopisto Teknillinen korkeakoulu
Aalto-universitetet Tekniska högskolan
Aalto University School of Science and Technology

Aalto University Publications in Materials Science and Engineering
Aalto-yliopiston materiaalitekniikan julkaisuja
Espoo 2010 TKK-MT-215

Densities of Molten and Solid Alloys of (Fe, Cu, Ni, Co) - S at Elevated Temperatures - Literature Review and Analysis

F. Tesfaye Firdu, P. Taskinen

Aalto University School of Science and Technology
Department of Materials Science and Engineering
Thermodynamics and Modeling of Metallurgical Processes (TDM)

Aalto-Yliopiston Teknillinen korkeakoulu
Materiaalitekniikan Laitos
Metallurgisten Prosessien Termodynamiikka ja Mallinnus (TDM)

Research program: ELEMET (Energy & Lifecycle Efficient Metal Processes)
Project: ISS (Improved Sulfide Smelting)
Financers: Boliden Harjavalta Oy, Boliden Kokkola Oy, Norilsk Nickel Finland Oy, Outotec Oyj and the Finnish Funding Agency for Technology and Innovation (Tekes)
Keywords: Density, thermal expansion coefficient, molar volume, alloy, Fe-S, Co-S, Ni-S, Cu-S

Distribution:
Aalto University School of Science and Technology
Department of Materials Science and Engineering
P.O. Box 16200
FI-00076 Aalto, Finland
Tel. +358 9 470 22796
Fax. +358 9 470 22798
E-mail: Fiseha.Tesfaye@tkk.fi

ISBN 978-952-60-3272-6
ISSN 1455-2329

Multiprint Oy
Espoo 2010

Abstract

Densities of solid and liquid Fe, Cu, Ni and Co, and their alloys both at the presence and absence of sulfur are reviewed. Volumetric thermal expansions were used to estimate the densities at different temperatures. Densities of the alloys generally decrease with increasing temperature. For the pure metals the reduction in density as temperature rises from 25^{o}C to their respective melting point may be generalized to be about 7.05 ± 0.4% just before melting and about 11.63 ± 0.92 on complete melting.

According to the literature data and analytic results, at ambient pressure, density of the stoichiometric FeS changes from 4.615 g/cm^3 at 25^{o}C to 3.8 g/cm^3 at 1200^{o}C (~17.7%), density of the stoichiometric Cu_2S changes from 5.65 g/cm^3 at 25^{o}C to ~5.18 g/cm^3 at 1200^{o}C (~8.3%), density of the stoichiometric NiS changes from 5.5 g/cm^3 at 25^{o}C to 5.025 g/cm^3 at 1027^{o}C (~8.5 ± 1.8 %) and density of the stoichiometric CoS changes from 5.45 g/cm^3 at 25^{o}C to 4.88 g/cm^3 at 1100^{o}C (~10.45%).

A study on the Fe-S melts at 4GPa suggests that in S-poor compositions, where solubility of sulfur is less likely to be affected by pressure, the density of the sulfides at isothermal conditions decreases in a similar fashion as under 1 bar, i.e., density decreases non-linearly with increasing sulfur.

Table of Contents

Abstract....4

Table of Contents....4

Symbols, Abbreviations, Units....6

1 Introduction....8

1.1 Estimation of Densities of Mixtures at Elevated Temperatures....8

1.2 High Temperature Densities of Fe, Co, Ni and Cu and Their Alloys....10

2 Densities of Solid Fe-, Co-, Ni- and Cu-Sulfides....15

3 Densities of Liquid Fe-, Co-, Ni- and Cu-Sulfides....19

3.1 Densities of Fe-S Melts....20

3.2 Densities of Ni-S Melts....23

3.3 Densities of Co-S Melts....24

3.4 Densities of Cu-S Melts....25

3.5 Densities of Melts in the Fe-Ni-Cu-S-(O) System....25

4 Effect of Pressure on Densities of the Sulfide Melts....28

5 Summary and Conclusions....29

Acknowledgements....29

References 30
Appendix A 32
Appendix B 33

Symbols, Abbreviations, Units

$\bar{\rho}$	average density	[g/cm^3]
X	bulk composition	
α	coefficient of linear thermal expansion	[K^{-1}]
β	coefficient of volumetric thermal expansion	[K^{-1}]
β_{liq}	coefficient of volumetric thermal expansion for a liquid phase	[K^{-1}]
β_{sol}	coefficient of volumetric thermal expansion for a solid phase	[K^{-1}]
x_i	composition of component i	
ρ	density	[g/cm^3]
ρ_x^L	density of pure/alloy liquid X	[g/cm^3]
ρ_x^S	density of pure/alloy solid X	[g/cm^3]
V^{Ex}	excess molar volume	[cm^3/mole]
T_{liq}	liquidus temperature	[K]
T_m	melting temperature	[K]
M	molar mass	[g]
V^m	molar volume	[cm^3/mole]
V_i	partial molar volume of component i	[cm^3/mole]
T_{tr}	phase transition temperature	[K]
T_{sol}	solidus temperature	[K]
T	temperature	[K]

1 Introduction

Specific gravity of a substance is primarily dependent on a substance's chemical composition and crystal structure, that is, by the kinds of atoms/ions present and the way they are packed and bonded. To generalize: the heavier the atom/ions, the higher the specific gravity; the closer the packing, the higher the specific gravity; and the stronger the bonding, the higher the specific gravity. Specific gravity also varies somewhat with varying temperature and pressure because changes in these conditions generally cause expansion or contraction. For instance the temperature and pressure conditions of formation of a mineral control its polymorphic form and thus the manner in which its constituent atoms/ions are packed [1].

Mathematical modeling has become an established tool for improving metallurgical processes. Accurate knowledge of physical properties of molten and solid phases is fundamentally important for many metallurgical processes. Density is required from simple mass balance calculations to the study of natural convection. The productivity and efficiency of many high-temperature processes rely on accurate knowledge of density, as well as the other physical properties, of alloys or their components at different temperatures. For instance, Density and its temperature dependence ($\frac{\partial \rho}{\partial T}$) are important parameters for simulation of solidification and flow behavior in the casting process of alloys, e.g., prediction of the defects such as microsegregation and gas porosity [2]. Other applications include: determination of settling phases in liquid mixtures like slags or in determining the settling rate of inclusions within molten mixtures.

1.1 Estimation of Densities of Mixtures at Elevated Temperatures

Molar volumes and masses of solid and liquid alloys can be expressed as the cumulative molar volumes and masses of each component of the solution (Vegard's law) as expressed in equations (1) and (2). Density of the mixture, which is the quotient of these two variables, is expressed by equation (3).

$$V^m = \sum_{i=1}^{n} x_i V_i \tag{1}$$

$$M = \sum_{i=1}^{n} x_i M_i \tag{2}$$

$$\rho = \frac{\sum_{i=1}^{n} x_i M_i}{\sum_{i=1}^{n} x_i V_i} \qquad \left(\sum_{i=1}^{n} x_i = 1\right) \tag{3}$$

The volumetric thermal expansion, experimentally determined thermodynamic property of a solution, is a unique property within a given temperature and composition ranges, at isobaric conditions. It's relation with temperature and molar volume, at an isobaric condition, is expressed as [3]:

$$\beta = \frac{1}{V^m}\left(\frac{\partial V}{\partial T}\right)_P = -\frac{1}{\rho^m}\left(\frac{\partial \rho}{\partial T}\right)_P \tag{4}$$

For exactly isotropic solid materials, the volumetric thermal expansion coefficient can be calculated from the linear thermal expansion coefficient (α) according to the relation in equation (5) [3].

$$\beta \approx 3 \cdot \alpha \quad (5)$$

Knowledge of the value of β would lead the determination of a new volume according to equations (6) and (7) [3].

$$V_{Solid} = V_{25°C}(1 + \beta_{sol}(T - 25°C)) \text{ (for solids)} \quad (6)$$

$$V_{liquid} = V_{mT_m}(1 + \beta_{liq}(T - T_m)) \text{ (for liquids)} \quad (7)$$

Using relations through (1) - (7) density of a material at a given temperature can be expressed as equations (8) and (9).

$$\rho_{Solid} = \rho_{25°C}(1 - \beta_{sol}(T - 25°C)) \quad \text{(for solids)} \quad (8)$$

$$\rho_{liquid} = \rho_{T_m}(1 - \beta_{liq}(T - T_m)) \quad \text{(For liquids)} \quad (9)$$

where V_{solid}, V_{liquid}, ρ_{solid}, ρ_{liquid} are volume and density of solids and liquids, respectively, β_{sol} and β_{liq} are coefficients of volumetric thermal expansion of solid and liquid phases, respectively. The density of materials as a function of temperature can also be estimated from experimentally determined coefficients A and B, as expressed in equation (10) [3].

$$\rho = A \cdot 10^3 - B \cdot T \quad (10)$$

Gibbs free energy change of a system generally expressed as [4]:

$$dG = -S \cdot dT + V^m \cdot dP + \sum \mu_i \cdot dx_i \quad (11)$$

For a closed system at an isothermal condition equation (11) can be written as:

$$V^m = \left(\frac{dG}{dP}\right)_{T,X} \quad (12)$$

which implies that,

$$G(P_2) - G(P_1) = \int_{p_1}^{p_2} V^m \cdot dP$$

Based on the nature of their compressibility, solids experience only a small change in their bulk volume for a pressure change ranging up to thousands of bars. For instance, most minerals' molar volume changes 3 – 4 % for pressure changes up to 40Kbar. That's why molar volume changes in industrial processes for certain pressure ranges are usually assumed to be zero. Increase in volume of the same amount can be expected for a change in temperature from 25 to 1000^{o}C [4].

molar volume of condensed phases', $V^m(T,P)$, can be generally expressed by the Murnaghan-equation [4]:

$$V^m(T,P) = \frac{V^m(T,0)}{(1+nK(T,0)\cdot P)^{1/n}} \quad (13)$$

where $V^m(T, 0)$ is molar volume at P = 0 (i.e., in a vacuum), K(T, 0) is isothermal compressibility at P = 0 and n is a constant which is obtained from isothermal bulk module as a function of pressure, according to equation (14) below [4].

$$B(T, P) = B(T, 0) + n\cdot P \quad (14)$$

where B(T, 0) is isothermal bulk module at P = 0 and P is the pressure condition under consideration.

1.2 High Temperature Densities of Fe, Co, Ni and Cu and Their Alloys

Experimental studies of several researchers show that density of materials either linearly or non-linearly declines with increasing temperature. A sharp fall in density of pure metals at a critical temperature of phase changes has also been reported by different researchers. For example, copper's molar density drops by about 4% on melting, as shown in Figure 1. Alloys exhibit a slower drop in density at the critical temperature of phase transitions. This is due to the mixed effect of the alloying elements. Densities of pure metals at temperatures (T'), above their respective melting temperatures, and the corresponding values for coefficients A and B in equation (10) are listed in Table 1.

Table 1. Liquid densities of pure Fe, Co, Ni and Cu (g/cm^3) and the corresponding coefficients A (T') and B (T') in equation (10) [3, 5]; experimental methods: M, maximum bubble pressure and S, sessile drop method.

Metal (T_m, K)	ρ_{T_m}	$\rho_{298.15K} - \rho_{T_m}$	$V_{T_m}^m$(cm^3)	A	B	T' (K)	Method
Co (1768.15)	7.75	1.11 (12.55%)	7.60	9.70	1.11	1793 - 1903	M
Cu (1357.75)	7.96	0.97 (10.86%)	8.09	8.75	0.66	1500 - 1898	M
Fe (1811.15)	7.03	0.84 (10.72%)	7.94	8.59	0.86	1812 - 1927	S
Ni (1728.15)	7.85	1.05 (11.80%)	7.42	10.1	1.27	1763 - 1933	M

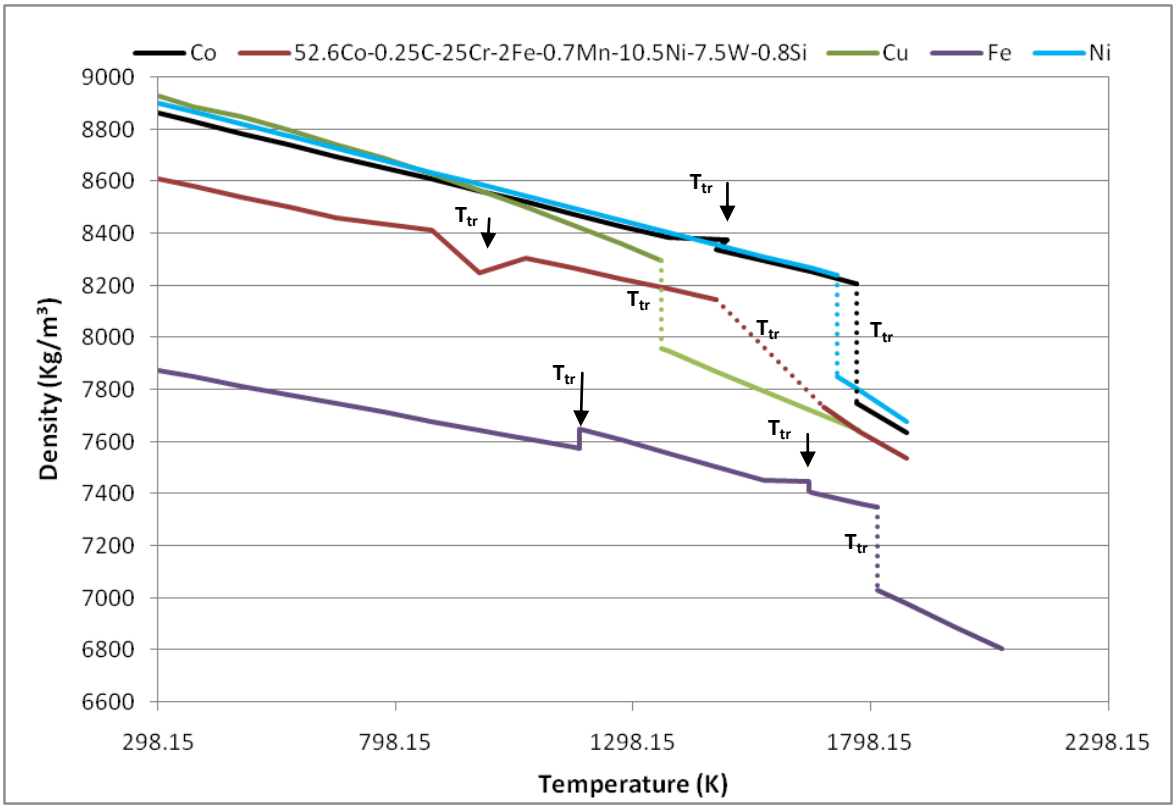

Figure 1. Densities of Fe, Co, Ni and Cu and their alloys as a function of temperature. Data adapted from [3].

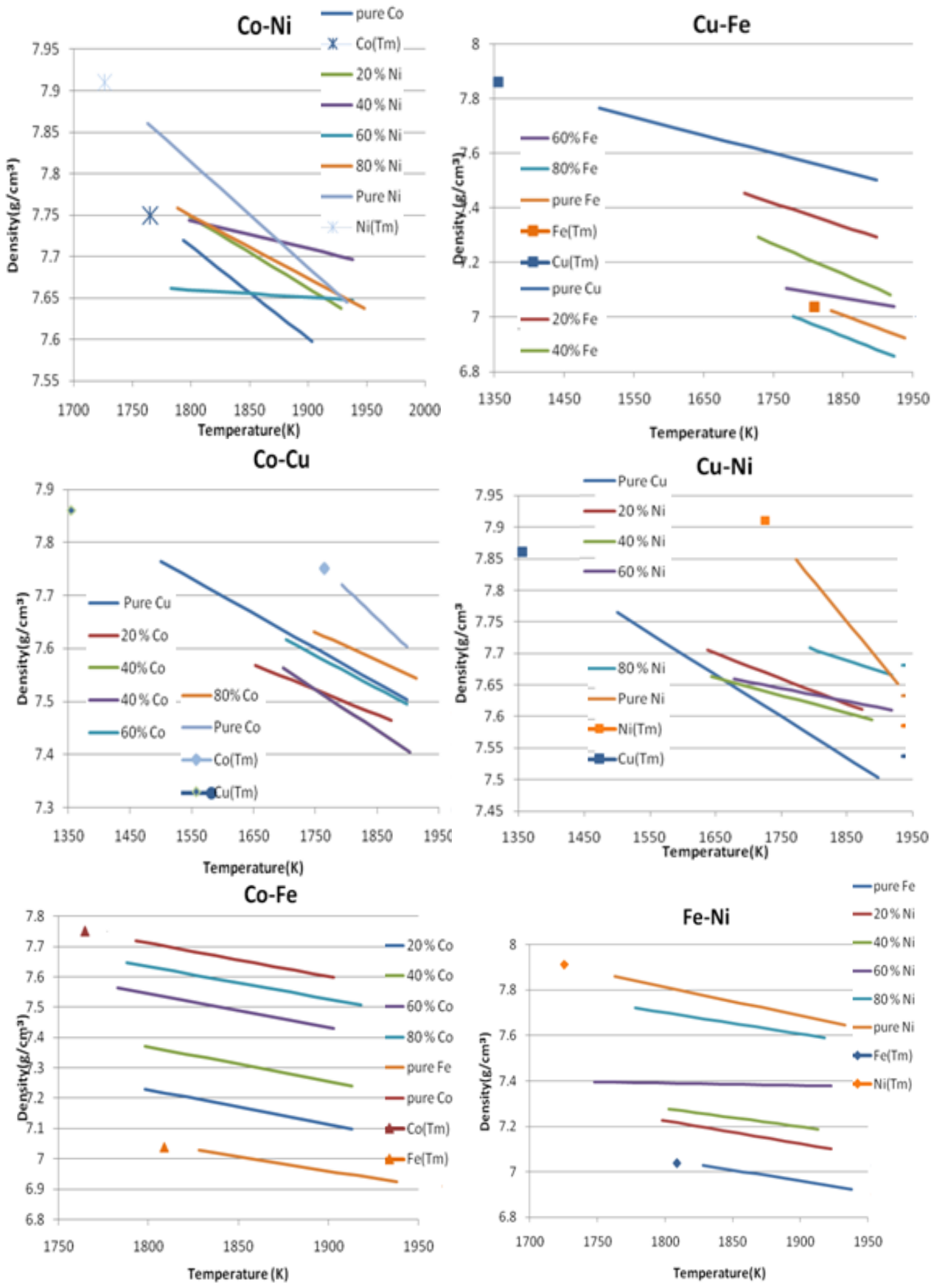

Figure 2. Density versus temperature diagram of liquid binary alloys of Fe, Co, Ni and Cu. Data (Appendix A) adapted from [5].

As shown in Figure 2 (a) - (f) density of the Cu-Fe-Co-Ni alloys increases with increasing amount of the heavier metal. For example, the density of the Cu-Fe alloys decreases with increasing fraction of Fe in the alloy.

Chemical elements in the Co-Ni-Cu system interacts in such a way that their alloys' density do not submit to the ideal condition in equation (3), as shown in Figure 2. Interaction of Fe with Co and Ni seems to have less effect on the density of the binary alloys. A similar effect has been reported by Birllo et al. [6], as illustrated in Figure 3 (a) and (b).

For a regular ternary solution with components i, each having the bulk concentration C_i, V is usually written as a function of temperature and concentrations [6]:

$$\mathrm{V}(\mathrm{C}_1, \ldots \mathrm{C}_3, \mathrm{T}) = \sum \mathrm{C_i V_i}(\mathrm{T}) + \mathrm{V^{Ex}}(\mathrm{C}_1, \ldots \mathrm{C}_3, \mathrm{T}) \qquad (15)$$

For an ideal mixing the second term in equation (15) vanishes and, thus, similar to the Vegard's law in equation (1). In the real case the excess term as a function of concentration and temperature is expressed as [6]:

$$\mathrm{V^{Ex}}(\mathrm{C}_1, \ldots \mathrm{C}_3, \mathrm{T}) = \sum_i^2 \sum_{j>i}^3 \mathrm{C_i C_j V_{i,j}^{Ex}} + \mathrm{C_1 C_2 C_3 V_T^{Ex}} \qquad (16)$$

The binary interaction parameter ($\mathrm{V_{i,j}^{Ex}}$) for Fe-Ni, Cu-Ni and Fe-Cu, at 1772K are 0, -0.85 and 0.6, respectively [6].

Table 2. Fitted parameters for density (g/cm^3), excess molar volumes (cm^3) and volumetric thermal expansion coefficients of Fe-Ni–Cu samples [7].

Composition	T (K)	β*10^{-5} (^{o}C^{-1})	ρ_L(T)	ρ(1773K)	V^{Ex}
$Ni_{40}Fe_{60}$	1725	1.6	7.43	7.39	~0
$Ni_{33}Cu_{13}Fe_{54}$	1692	0.4	7.11	7.09	0.34
$Ni_{25}Cu_{40}Fe_{35}$	1610	1.1	7.14	7.01	0.53
$Ni_{20}Cu_{50}Fe_{30}$	1591	0.5	7.20	7.14	0.39
$Ni_{16}Cu_{60}Fe_{24}$	1580	2.6	7.53	7.16	0.4
$Ni_{17}Cu_{70}Fe_{13}$	1546	1.5	7.76	7.51	0.06
Cu	1358	1	7.89	7.58	-
$Ni_{15}Cu_{20}Fe_{65}$	1701	2	7.16	7.05	0.28
$Ni_{32}Cu_{20}Fe_{48}$	1669	2.3	7.40	7.23	0.22
$Ni_{45}Cu_{20}Fe_{35}$	1663	1.4	7.42	7.3	0.25
$Ni_{60}Cu_{20}Fe_{20}$	1668	1.1	7.56	7.47	0.19
$Ni_{70}Cu_{20}Fe_{10}$	1673	1.1	7.79	7.71	0.02

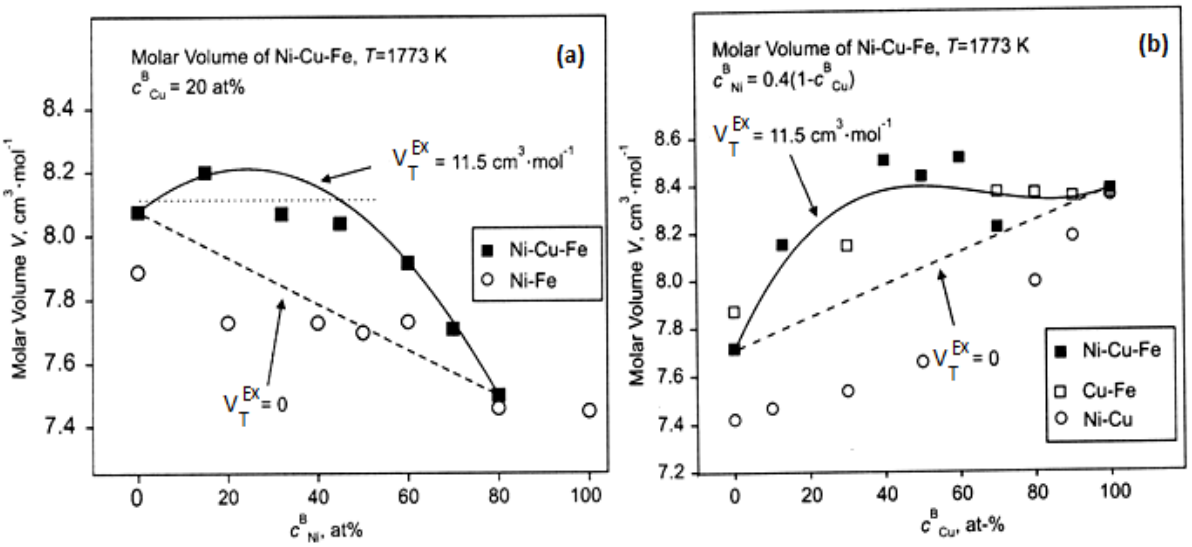

Figure 3. (a) Molar volume, V^m, of Ni-Cu-Fe, samples from section A in Figure 4 (b), at 1773K, (b) Molar volume, V^m, of Ni-Cu-Fe, samples from section B in Figure 4 (b), at 1773K. In both diagrams the interaction parameter of the ternary was obtained as a result of fitting curves to experimental points according to equation (16) [6].

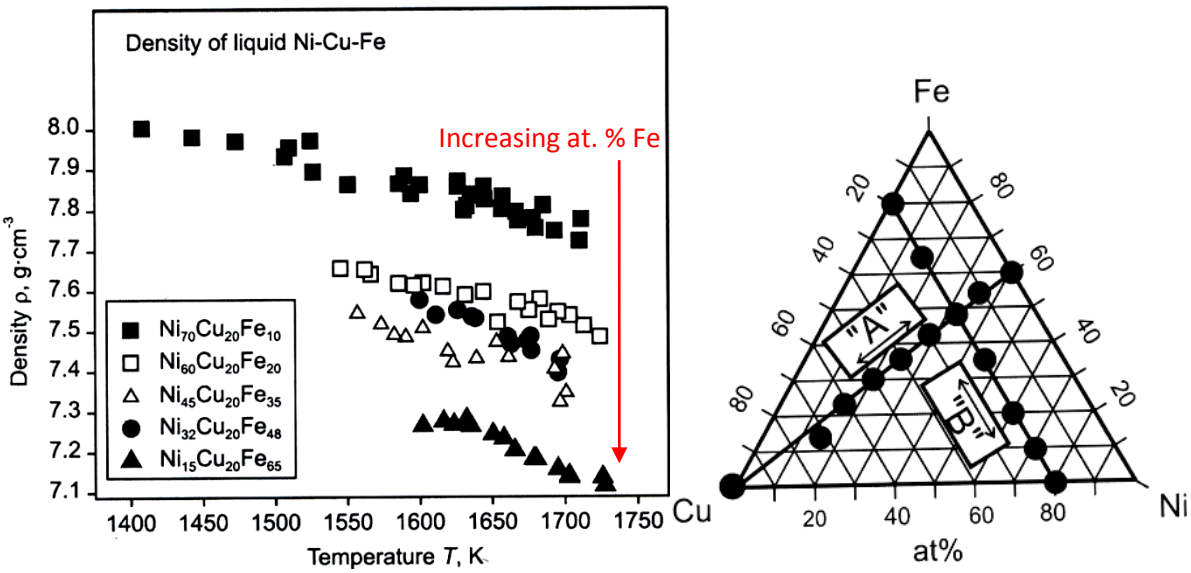

Figure 4. Densities of liquid Fe-Co-Ni alloys as a function of temperature, along the line B in (b), (b) composition of the samples used in the density and molar volume calculations [6].

Figure 4 shows the decrease in the density of the Fe-Ni-Cu liquid mixtures, at a fixed amount of Cu (20 at. %), as the temperature and fraction of Fe increases.

2 Densities of Solid Fe-, Co-, Ni- and Cu-Sulfides

The coefficient of thermal expansion measures the fractional change in volume per degree Celsius change in temperature at a constant pressure. All substances expand or contract when their temperature change, and the expansion or contraction always occurs in all directions. Unlike gases or liquids, solid materials tend to keep their shape, though they expand as temperature rises.

Table 3. Densities of some sulfides and sulfosalts at 25^{o}C [1, 8, 9, 10, 11, 12, 13] (g/cm^3).

Metal(M)	Ore Mineral	Chemical formula	wt. % M	ρ	$\bar{\rho}$
Cu	Chalcopyrite	$CuFeS_2$	34.62	4.1 - 4.3	4.2
	Chalcocite	Cu_2S	79.85	5.5 - 5.8	5.65
	Bornite	Cu_5FeS_4	63.31	4.9 - 5.4	5.15
	Covellite	CuS	66.46	4.6	4.6
	Tennantite	$Cu_8As_2S_7$ (variable)	57.59	4.4 - 4.5	4.45
	Enargite	Cu_3AsS_4	48.41	4.4	4.4
	Tetrahedrite	$4Cu_2S{\cdot}Sb_2S_3$	52.10	4.4 - 5.1	4.75
		$Cu_{12+x}Sb_{4+y}S_{13}$ $0.11<x<1.77$, $0.03<y<0.3$	-	5.1 ± 0.075	5.1
		$Cu_{12.3}Sb_{4+}S_{13}$	-	5	5
		$Cu_{10}Fe_2Sb_4S_{13}$	-	4.81	4.81
Ni	Pentlandite	(Fe,Ni)S	22.00	6 - 5.0	4.8
	Niccolite	NiAs	44.10	7.3 - 7.7	7.5
	Millerite	NiS	64.80	5.3 - 5.7	5.5
Fe	Troilite	FeS	63.53	4.58 - 4.65	4.615
	Pyrrhotite	$FeS(Fe_{0.95}S)$	62.33	4.58 - 4.65	4.615
	Pyrite	FeS_2 (Isometric)	46.55	4.9 - 5.2	5.05
	Marcasite	FeS_2 (Orthorhombic)	46.55	4.887	4.887
	Arsenopyrite	FeAsS	33.3	6.10	6.10
Zn	Sphalerite	ZnS	67.1	3.9 - 4.1	4.0
Co	Smaltite	$CoAs_2$	28.22	5.7 - 6.8	5.75
	Cobaltite	CoAsS	35.52	6 - 6.3	6.15
	Carrolite	$CuCo_2S_4$	20.52	4.8 - 5.0	4.9
	Linnaeite	Co_3S_4	57.96	4.8 - 5.0	4.9
Pb	Galena	PbS	86.60	7.4 - 7.6	7.5
Sb	Stibnite	Sb_2S_3	71.8	4.5 - 4.6	4.55
As	Arsenopyrite	FeAsS	46.00	5.9 - 6.2	6.05
	Realgar	AsS	70.03	3.5	3.5
	Orpiment	As_2S_3	60.90	3.4 - 3.5	3.45
Bi	Bismuthinite	Bi_2S_3	81.2	6.8	6.8

Using equation (8) and thermal expansion coefficients in Table 4, density of a sulfide/sulfosalt, within the temperature limits, can be expressed as:

$$\rho_{Solid} = \rho_{lm}(1 - \beta_{sol}(T_{uul} - T_{lm})) \quad (17)$$

where ρ_{lm}, T_{uul}, T_{lm} are density at the lower temperature limit, temperatures under the upper limit and the lower temperature limit, respectively.

Using the thermal expansion coefficients in Table 4 the density of the pyrrhotite (FeS), according to equation (17), varies from 4.615 at 25^{o}C to 4.543 at 140 ^{o}C and 4.237 at 320^{o}C, as illustrated in Figure 5.

Table 4. Thermal expansion coefficients of some sulfides ($^{o}C^{-1}$), ($\beta = 3 \cdot \alpha$).

Mineral	Composition	T (^{o}C)	$\alpha*10^{-5}$($^{o}C^{-1}$)	$\beta*10^{-5}$	Ref.
Troilite	FeS	300 – 600	7.4	22.2	[14]
		100 – 300	14.1	42.3	[14]
Pyrite	FeS_2	20 – 100	2.1	6.3	[15]
		20 – 200	2.9	8.7	[15]
		20 – 300	1.1	3.3	[15]
Pyrrhotite	FeS	25 – 140	4.5	13.5	[15]
	FeS	140 – 320	12.5	37.5	[15]
	$Fe_{0.923}S$	75 – 320	12.6	37.8	[15]
	$Fe_{0.875}S$	25 – 292	9.0	27	[15]
Ni-rich pyrrhotite	$Fe_{0.84}Ni_{0.11}S$	300 – 600	8.0	24	[14]
		100 – 300	9.3	27.9	[14]
Ni-poor pyrrhotite	$Fe_{0.87}Ni_{0.02}S$	300 – 600	8.5	25.5	[14]
		100 – 300	8.4	25.2	[14]
Pentlandite (Outokumpu)	-	24 – 235	3.9	11.7	[15]
	-	24 – 350	5.8	17.4	[15]
Pentlandite (Frood)	-	24 – 200	20.6	61.8	[15]
	-	24 – 200	11.1	33.3	[15]
Pentlandite (Synthetic)	-	25 – 220	15.1	45.3	[15]
Digenite	$Cu_{1.8 + X:(0 – 0.2)}S$	409.85 – 654.85	-	3.2-5.49	[16]
Covellite	CuS	119.85 - 339.85	-	2.42	[16]
Tetrahedrite (synthetic)	$Cu_{12(..13.9)}Sb_4S_{13}$	100-250	~14.3	42.9	[11]

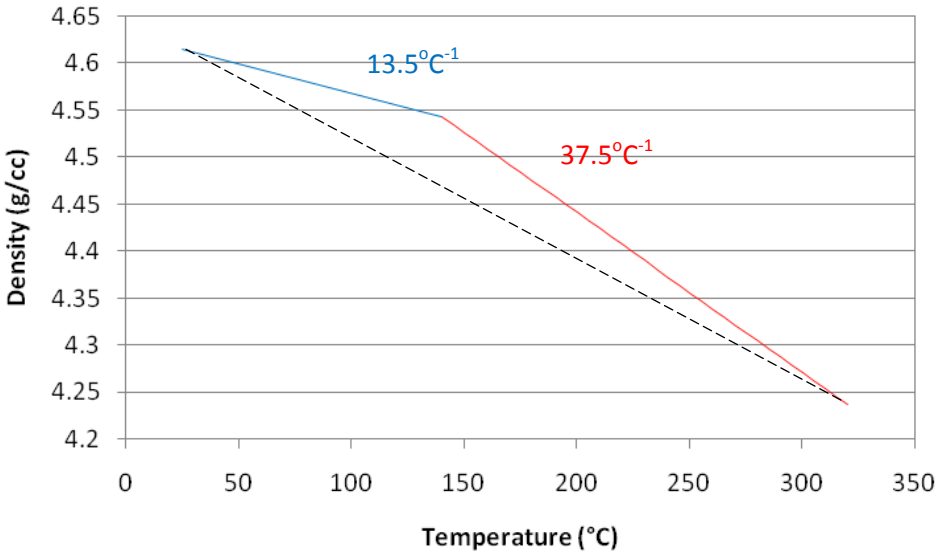

Figure 5. Density of the pyrrhotite ($Fe_{1-x}S$) as a function of temperature. Calculated using equation (17) based on volumetric thermal expansion coefficients in Table 4 and density at room temperature in Table 3.

For multi-component sulfides density varies significantly based on the mass of a component that has replaced the other component. As shown in Figure 6, the replacement of a heavier atom Cu by a lighter atom Fe causes decrease in the density of the structure.

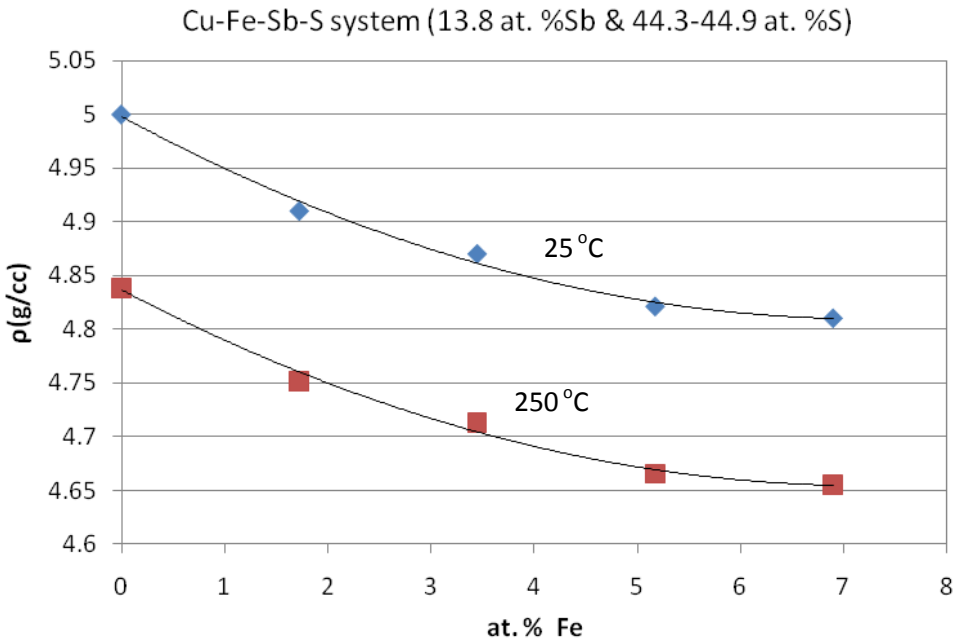

Figure 6. For a fixed amount of Sb and S the effect of increase in the amount of Fe, with respect to Cu, on density of the sulfosalt; data at 25°C is adapted from [17].

The density of the Cu-Fe-Sb-S system at constant concentration of sulfur and antimony (13.8 at. % Sb and ~44.6 at. % S) and substitution of Cu by Fe can be approximated as:

$$\rho(298.15℃) = 0.0036 \cdot (at.\%\, Fe)^2 - 0.0519 \cdot (at.\%\, Fe) + 4.9973 \qquad (18)$$

Using the volumetric thermal expansion of tetrahedrite ($Cu_{12(..13.9)}Sb_4S_{13}$) in Table 4 and extending the lower temperature limit to the room temperature (since nearly the same α was reported by Karen et al. [18] for $Cu_{11.4}Fe_{0.6}Sb_4S_{13}$ in the temperature rage 25-250^{o}C), density of the sulfosalt at 250^{o}C can be expressed by equation (19).

$$\rho(1273.15℃) = 0.0035 \cdot (at.\%\, Fe)^2 - 0.0502 \cdot (at.\%\, Fe) + 4.8365 \qquad (19)$$

3 Densities of Liquid Fe-, Co-, Ni- and Cu-Sulfides

By measuring the densities of metallic alloys, Zushu et al. [19] reported that they observed about 6 % difference from calculated values, which assumed ideal mixing. Highly negative departure from the ideality (Raonalt's law) would mean tighter bond among the alloying elements and a denser structure for the bulk. Thus, molar volume of the alloys should be expressed as equation (20) [19].

$$V^m = \Sigma x_i V_i + V^{Ex} \quad (20)$$

where V^{Ex} is the excess molar volume that results in deviation from the ideal one. Density can also be re-expressed as:

$$\rho^m = \Sigma x_i \rho_i + \rho^{Ex} \quad (21)$$

Density measurements of metallic sulfides, at the presence of oxygen, indicate both positive and negative deviations from linear mixing of partial molar volumes [20]. Thus, the excess term can be a positive or negative based on the interactions among the solution making components.

The partial molar volume of components depends on the condition of the solution. As a result of least square fitting, Nagamori [21] obtained parameters in Table 6 and 7 and equations (22) and (23) to estimate partial molar volumes and molar volumes of the Cu-S, Fe-S and Ni-S melts, respectively.

$$V_i \left(\frac{cc}{mol}\right) = a^i + b^i X_S - c^i X_S^2 \quad (22)$$

$$V^m \left(\frac{cc}{mol}\right) = a + bX_S + cX_S^2 \quad (23)$$

Table 5. Partial molar volumes in the Fe-S, Ni-S and Cu-S melts at infinite dilution [21].

System	T(K)	V_S(cm^3/mol)	V_M(cm^3/mol)
Fe-S	1473.15	12.1	7.7
Ni-S	1373.15	10.6	7.1
Cu-S	1473.15	14.8	8.0

Table 6. Values of parameters a, b and c in equation (23) for molar volume calculation of the Fe-S, Ni-S and Cu-S melts [21].

System	T(K)	Composition	a	b	c	Accuracy
Fe-S	1473.15	$0.40 < X_S < 0.51$	13.69	-28.99	49.38	± 0.6
Ni-S	1373.15	$0.28 < X_S < 0.44$	9.96	-16.09	34.05	± 0.5
Cu-S	1473.15	$0.326 < X_S < 0.343$	8.01	6.67	-	± 0.5

Table 7. Values of parameters a^i, b^i and c^i in equation (22) for partial molar volume calculations of the components in the Fe-S, Ni-S and Cu-S melts [21].

System	T(K)	Components	a^i	b^i	c^i	Accuracy
Fe-S	1473.15	S	-15.3	98.76	49.38	± 0.5
		Fe	13.69	-	49.38	± 0.5
Cu-S	1473.15	S	14.8	-	-	± 1
		Cu	8	-	-	± 1
Ni-S	1373.15	S	-6.13	68.10	34.05	± 0.5
		Ni	9.96	-	34.05	± 0.5

Using the experimentally obtained coefficients in Table 6 and 7, it is possible to calculate the excess terms of the melts at 1200 and 1100°C. The partial molar volume of components of a mixture at elevated temperatures varies with the amount of components in the mixture. For example, the partial molar volume of sulfur (at X_S=0.35) in the Ni-S melts is about 13.53 cm^3/mol whereas its value at infinite dilution is 10.6, as shown in Table 5.

3.1 Densities of Fe-S Melts

If a symmetric regular solution is assumed for Fe-S liquids the molar volume can be expressed as [22]:

$$V^m = V_{Fe}X_{Fe} + V_S X_S + \psi X_{Fe} X_S \quad (24)$$

$$V^{Ex} = V^m - V^{id} \quad (25)$$

where X_{Fe} and X_s are Fe and S contents in atomic ratios and ψ experimentally determined coefficient of the excess term. The last term in equation (24) expresses the excess molar volume. Nichida et al. [22] illustrated the extent of this excess term in Figure 7 below.

Based on experimental results, Mietinen et al. [23] estimated equations (26) and (27) to model the densities of liquid Fe-Sulfides, as a function of temperature (1100 – 1500°C) and composition, at ambient pressure.

$$\rho_{Fe-S}\left(\frac{Kg}{m^3}\right) = 8319.49 - 0.835 \cdot (T - 273.15) + a_s C_S \quad (26)$$

$$a_s = -82.18 + 0.005571 \cdot (T - 273.15) - 0.673970 \cdot C_S \quad (27)$$

where C_S is composition of S in wt. %.

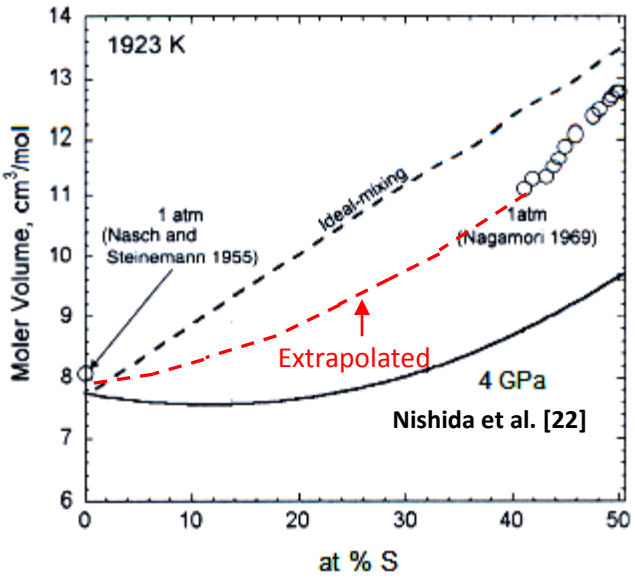

Figure 7. Variation of V^m with sulfur content at 1925K and 4Gpa; the open circles represent molar volumes at 1923K (at ambient pressure) [22].

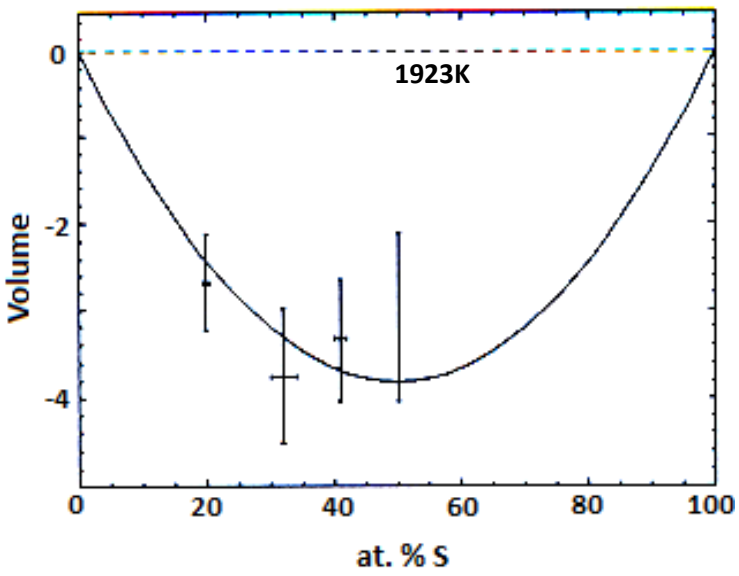

Figure 8. Excess molar volume of Fe and S at 4 Gpa; each crossed point represents the excess molar volume calculated using equation (24), the solid curve shows V^{Ex} at ψ = -15.24 [22].

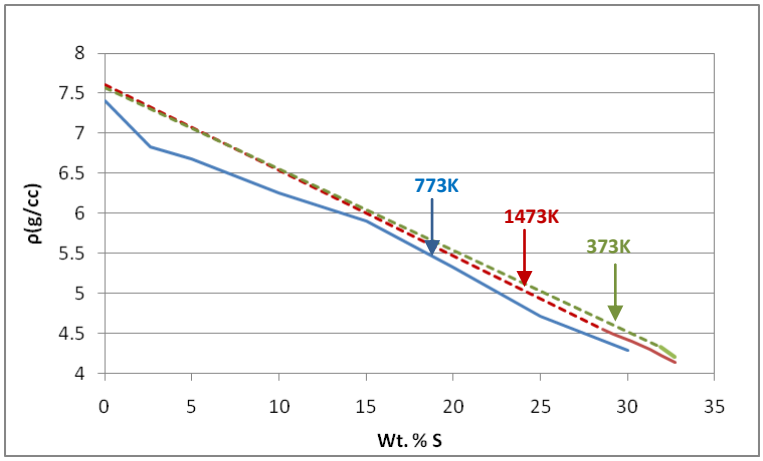

Figure 9. Density of the Fe-S melts as a function of mass percent of S; density decreases linearly with the increasing fraction of S and increases only with temperature; dashed lines are extrapolated assuming ideal mixing. Data adapted from Miettinen et al. [23].

Assuming that species' partial molar volumes are constant at a given T and P, component partial molar volumes are a function of the bulk composition, resulting in a positive deviation from linear component mixing of volumes. For instance, S^{2-} has a molar volume of about 18.2 cm^3/mol (Table 8), however, in a Ag-S melts Nagamori [21] reported that it is about 15.3 cm^3/mol and in Cu-S melts it is about 14.8 cm^3/mol. The reduction in volume of S^{2-} in Cu-S melts with respect to the Ag-S melts may be interpreted as the presence of more covalently bonded sulfur or non localized electrons. According to the electronegativity values the Ag-S is more ionic than that of Cu-S bonding. Thus, the partial molar volume of sulfur in sulfides may increase with ionic bonding [21].

Table 8. Molar volumes of pure elements and liquid sulfides at 1300K (with 2.5% average error) [20]; densities are calculated using equation (3).

Species	Molar volume (cm^3/mole)	ρ(calculated)
S	14.45	2.219
S^{2-}	18.2(15.4) (Nagamori [21])	-
Fe	7.68	7.272
Ni	7.23	8.119
Cu	7.89	8.054
FeS	22.20	3.960
NiS	18.06	5.025
CuS	17.77	5.380

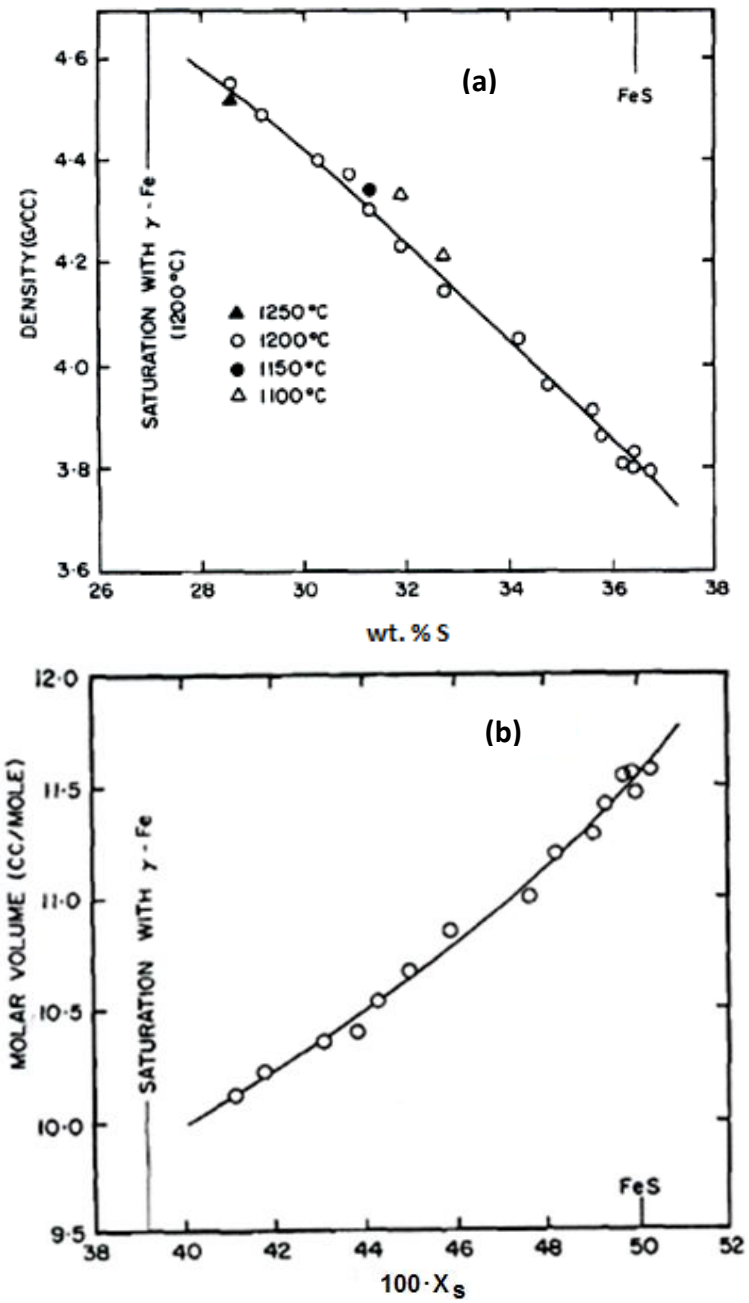

Figure 10. (a) Densities of the Fe-S melts, at different temperatures, as a function of sulfur content, (b) molar volumes of the Fe-S melts at 1200°C as a function of composition [21].

Densities of the Fe-S melts at 1200°C and 28 < [wt. % S] < 37 can be estimated by equation (24) fitted from experimental data [21] as:

$$\rho_{Fe-S}(g/cc) = 6.95 - 7.523 \cdot 10^{-2} \cdot (wt.\,\%\,S) - 2.997 \cdot 10^{-4} \cdot (wt.\,\%\,S)^2 \pm 0.025 \qquad (28)$$

3.2 Densities of Ni-S Melts

As a result of experimental work, Nagamori [21] suggested that a temperature coefficient of the Ni-S melts, in the temperature range 1000-1200°C and 18 < [wt. % S] < 30, can be estimated by equation (29).

$$d\rho_{Ni-S}/_{dT} = -2.4 \cdot 10^{-3} + 8 \cdot 10^{-5} \cdot (wt.\%\, S) \quad (29)$$

At 1200°C and 18 < [wt. % S] < 30 the densities of Ni-S melts may be calculated by equation (30) below [21]:

$$\rho_{Ni-S}(g/cc) = 7.24 - 2.254 \cdot 10^{-2} \cdot (wt.\%\, S) - 17.95 \cdot 10^{-4} \cdot (wt.\%\, S)^2 \pm 0.03 \quad (30)$$

According to the experimental data the density of the stoichiometric Ni_3S_2 is calculated as (with an error of ± 0.04 g/cm^3):

$$\rho_{Ni_3S_2} = 5.41 - 3 \cdot 10^{-4} \cdot (T - 1000) \quad (31)$$

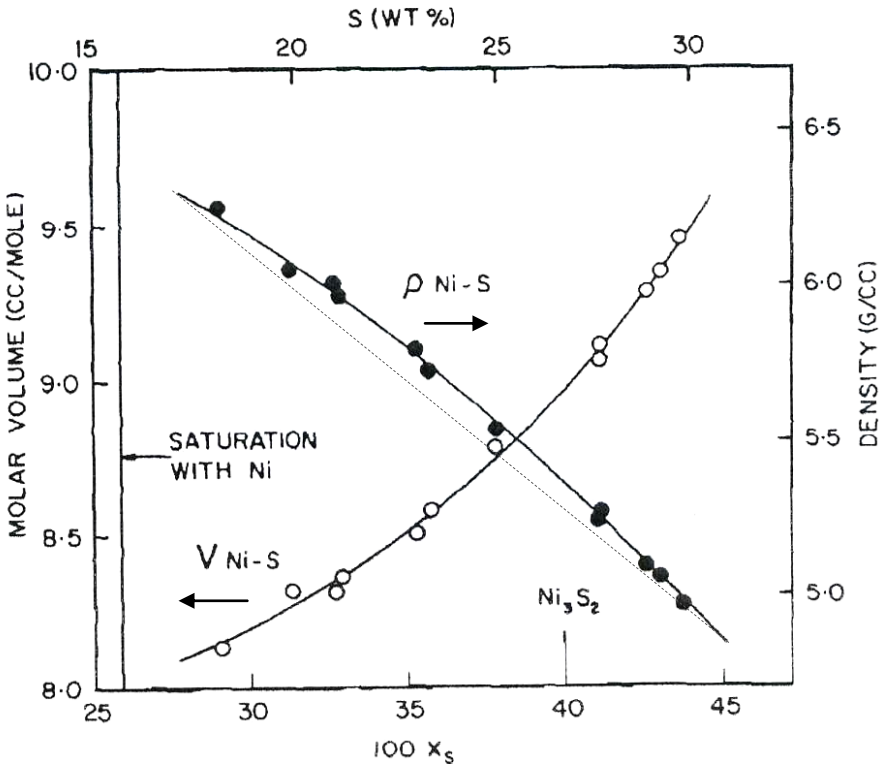

Figure 11. Densities and molar volumes of the Ni-S melts at 1100°C as a function of composition [21].

As shown in Figure 11, the densities of Ni-S melts deviate positively from the densities assuming ideal mixing.

3.3 Densities of Co-S Melts

Taking the partial molar volume of Co at 1100°C from Figure 1 (7.03 cm^3/mol) and that of S from Table 6 (13.53 cm^3/mol, partial molar volume of S in Ni-S melts at X_S=0.35) and assuming ideal mixing, molar volume of the Co-S melts, at 1100°C, may be estimated from relations in equation (32) below.

$$V^m_{Co-S} = X_{Co} \cdot 7.03 + X_S \cdot 13.53 \quad (32)$$

Using equation (32), the density of the CoS melt, at 1100°C, is about 5.31 g/cm^3 (5.45 at 25°C [10]). Considering the excess term to be equal to that of the Ni-S melts (at 1100°C and X_S=0.35) density of CoS is about 4.88 g/cm^3.

3.4 Densities of Cu-S Melts

The experimental work of Nagamori [21] shows that the density and molar volume of molten Cu-S melts, at 1200°C, can be expressed as:

$$V^m_{Cu-S}(cc/mol) = 8.01 + 6.76X_S \pm 0.05 \quad \text{(For 19.6 < [wt. \% S] < 20.6)} \quad (33)$$

$$\rho_{Cu-S}\left(\frac{g}{cc}\right) = 7.9 - 13.48 \cdot 10^{-2} \cdot (wt.\%\, S) \pm 0.15 \quad (34)$$

According to equation (34), the density of Cu_2S at 1200°C is 5.184 ± 0.15, which is in agreement with the value listed in Table 9.

3.5 Densities of Melts in the Fe-Ni-Cu-S-(O) System

Figure 12 includes three plots of the density versus sulfur content for sulfide liquids, close to the Fe–S, Ni–S and Cu – S binaries.

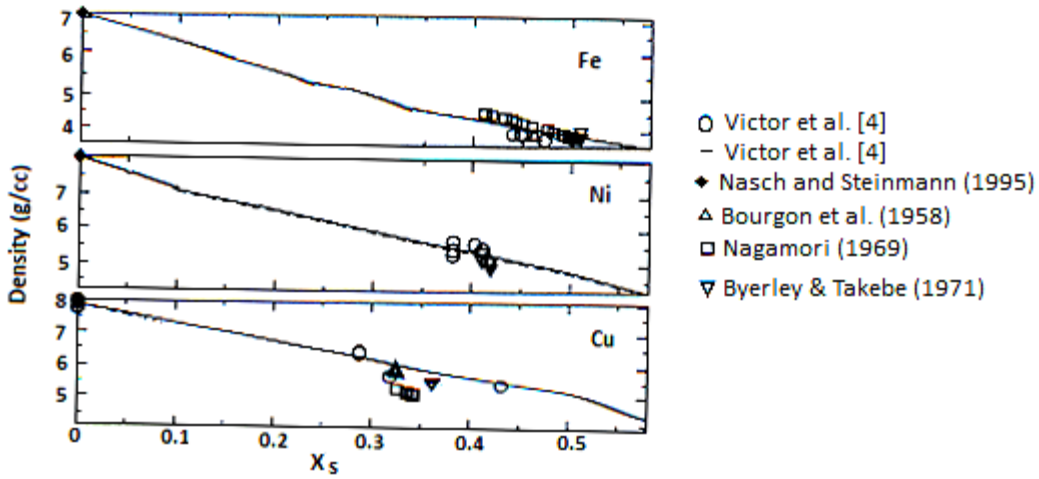

Figure 12. Densities of liquids in the Fe–S, Ni–S and Cu–S binaries; experimental results between 1201°C and 1299°C in which mol. % O is less than 5 are included [20].

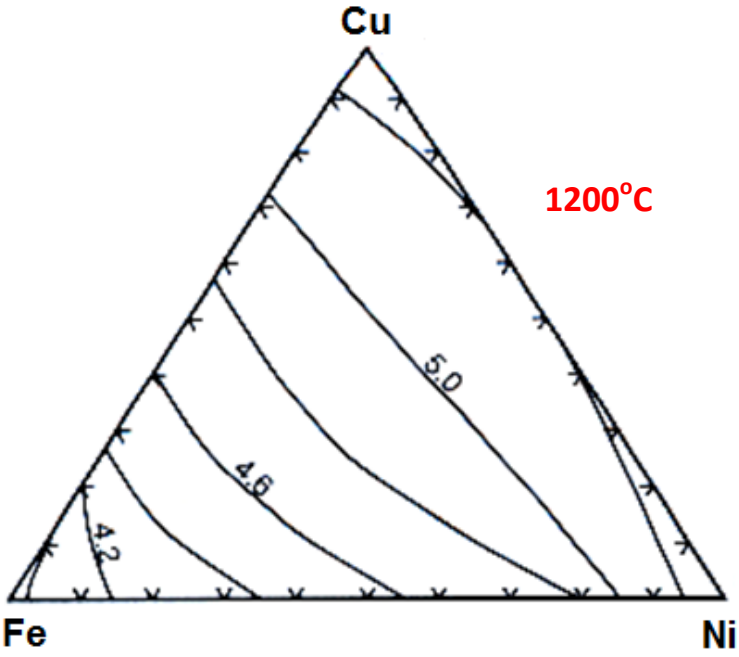

Figure 13. A Plot of the calculated density of sulfide liquids at 1200°C, $log_{10}^{f_{O_2}}$= - 8.68 and $log_{10}^{f_{S_2}}$ = - 2 [20].

The 35% density difference between Ni-S-(O) liquids (5.33 g/cm^3) and Fe-S-(O) liquids (3.96 g/cm^3) under the conditions shown in Figure 13 is much larger than the 11% density difference between the densities of liquid Ni (8.356 g/cm^3, Figure 14) and liquid Fe (7.503 g/cm^3, Figure 15). Density difference between the Fe(l) and Fe-S-O liquids is larger than that of the difference between the Ni(l) and Ni-S-O liquids. This may be as a result of higher equilibrium oxygen contents and anion/cation ratios in the Fe-S-O liquids than in the Ni-S-O liquids. Thus, the effect of oxygen on the densities of sulfides is expected to be more significant in Fe-rich compositions [20].

Table 9. Densities of sulfide melts [21, 24, 25] (g/cm^3).

Composition	~T_m(K)	T(K)	ρ (T)	Ref.
FeS	1468.15	~1473.15	3.90	[24]
FeS	1468.15	1473.15	3.80	[21]
FeS	1460	1500	3.80	[25]
Cu_2S	1403.15	~1473.15	5.20	[24]
Cu_2S	1403.15	1473.15	5.18	[21]
Cu(79.70 wt. %)S(20.30 wt. %)	-	1473.15	5.15 ± 0.02	[21]
Cu_2S-FeS (50 wt. % Cu)	1310	1500	4.30	[25]
Cu_2S-FeS (80 wt. % Cu)	1400	1500	5.80	[25]
Ni_3S_2	-	1373.15	5.36	[21]
Bi_2S_3	1033.15	1073.15	6.03	[21]
Ag_2S	1098	1423.15	6.37	[21]

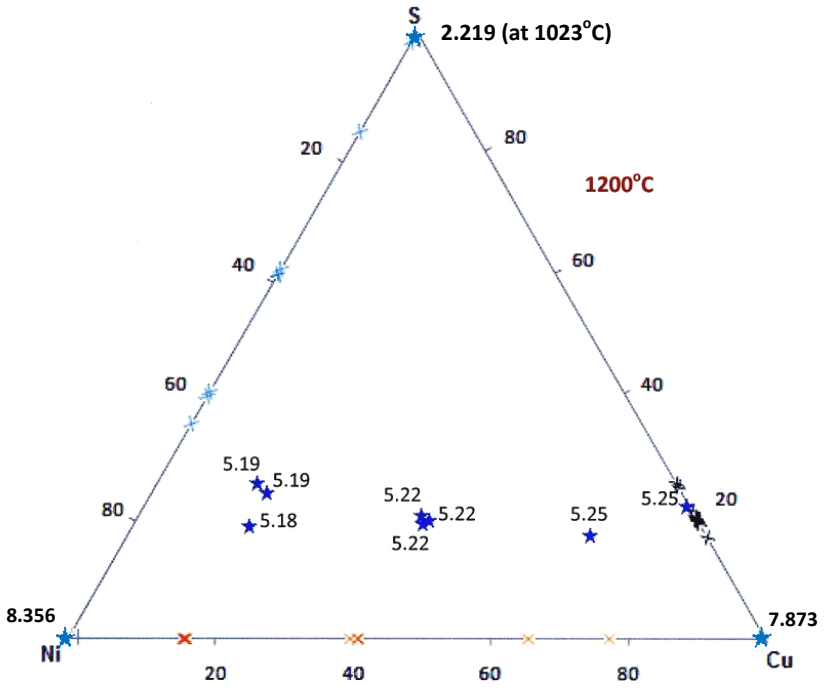

Figure 14. Isothermal density diagram for some compositions in the Ni-Cu-S system. Solid stars show densities at 1200°C; the data (Appendix B) were adapted from the experimental work of Toguri et al. [26] (g/cm^3).

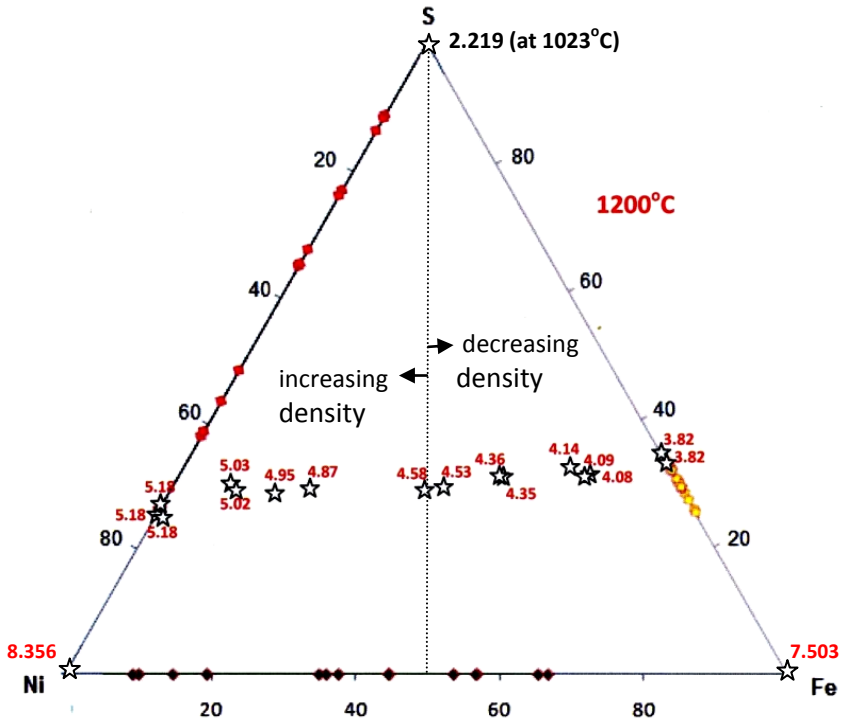

Figure 15. Isothermal density diagram for some compositions in the Ni-Fe-S system. Open stars show densities at 1200°C; the data (Appendix B) were adapted from the experimental work of Toguri et al. [26] (g/cm^3).

4 Effect of Pressure on Densities of the Sulfide Melts

Conditions of high pressure favor formation of polymorphic forms with high densities, whereas conditions of high temperature favor looser packing and formation of polymorphic forms with relatively low densities [1]. As in the case of ambient pressure conditions, the densities of Fe–S melts decrease non-linearly with increasing sulfur content at 4 GPa and 1923 K, as depicted in Figure 16. The excess molar volumes of Fe and S at 4 GPa deviate negatively from the ideal molar volume. In general, the change in the molar volumes (V^m) and the excess molar volumes (V^{Ex}) with sulfur content at high pressures, at least up to 4 GPa, is similar to that of ambient pressure conditions [22]. As Figure 16 shows, however, at higher sulfur content the variation in the densities at 4GPa and 1atm grows.

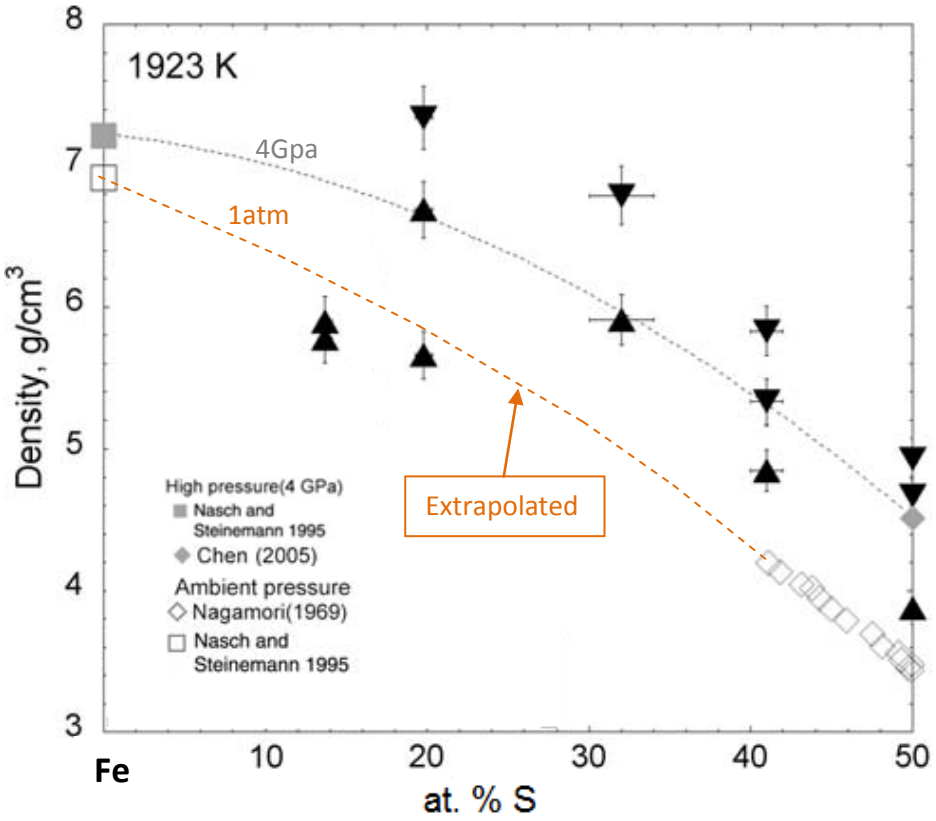

Figure 16. A modified sulfur content versus density of liquid Fe–S diagram, originally calculated by Nishida et al. [22]. The open diamonds represent the density of liquid Fe–S at ambient pressure and 1923 K derivative (dq/dT) of $8 \cdot 10^{-4}$ from 1473 K (Nagamori (1969) [21]). The open squares represent the density at ambient pressure and 1923 K (Nasch and Steinemann 1995). Black downward- and upward-pointing triangles represent measured densities of the Fe–S samples. The dotted bold line in this area shows the density of Fe–S liquids with various sulfur contents decreasing monotonically. The gray square represents the calculated values at 4 GPa and 1923 K based on the elastic parameters of liquid Fe obtained by Nasch and Steinemann (1995). The gray diamod represents the density of liquid FeS at 4.1 GPa (measured by Chen (2005) and using Nagamori's [18] data: dq/dT = $8 \cdot 10^{-4}$).

5 Summary and Conclusions

Densities of solid and liquid Fe, Cu, Ni and Co, and their alloys both at the presence and absence of sulfur are reviewed. Volumetric thermal expansions were used to estimate the densities at different temperatures. Densities of the alloys generally decrease with increasing temperature. For the pure metals the reduction in density as temperature rises from 25^{o}C to their respective melting point may be generalized to be about 7.05 ± 0.4% just before melting and about 11.63 ± 0.92 on complete melting.

According to the literature data and analytic results, at ambient pressure, density of the stoichiometric FeS changes from 4.615 g/cm^3 at 25^{o}C to 3.8 g/cm^3 at 1200^{o}C (~17.7%), density of the stoichiometric Cu_2S changes from 5.65 g/cm^3 at 25^{o}C to ~5.18 g/cm^3 at 1200^{o}C (~8.3%), density of the stoichiometric NiS changes from 5.5 g/cm^3 at 25^{o}C to 5.025 g/cm^3 at 1027^{o}C (~8.5 ± 1.8 %), and density of the stoichiometric CoS changes from 5.45 g/cm^3 at 25^{o}C to 4.88 g/cm^3 at 1100^{o}C (~10.45%).

At isothermal and isobaric conditions, densities of the sulfides decrease with increasing fraction of sulfur. If a sulfide contains more than one metal, the density decreases with increasing concentration of the lighter metal, at fixed amount of sulfur. Interaction of the alloy forming components determine the excess terms in the molar volume alloys. The molar volume may deviate positively or negatively from the ideal molar volume resulting in nonlinear ρ-X-T relations. As the fraction of sulfur increases the V^m(sulfides) deviate negatively from ideal-mixing and/or the respective ρ^m values deviate positively from the ideal-mixing. However, at the presence of oxygen this might not hold.

A study on the Fe-S melts at 4GPa suggests that in S-poor compositions, where solubility of sulfur is less likely to be affected by pressure, the density of the sulfides at isothermal conditions decreases in a similar fashion as under 1 bar, i.e., density decreases non-linearly with increasing sulfur.

Acknowledgements

The authors are grateful to Improved Sulfide Smelting (ISS) project of the ELEMET program and Tekes, the Finnish Funding Agency for Technology and Innovation, for financial support. This work was made as a sub task of ISS, supported financially by Boliden Harjavalta Oy, Boliden Kokkola Oy, Norilsk Nickel Finland Oy and Outotec Oyj.

References

1. Berry, Mason D. Mineralogy, 2nd edition. 1983. 551 p. ISBN 0-7167-1424-8.
2. Fang, L., Xiao, F., Wang, Y.F., Tao, Z.N., MuKaic, K. Density and molar volume of liquid Ni-Co binary alloys. Materials Science and Engineering B 132. 2006. pp. 174 – 178.
3. Mills, Kenneth C. Recommended values of Thermophysical Properties for Selected Commercial Alloys. NPL & ASM International. 2002. 244 p.
4. Taskinen, P. Realisystemien termodynamiikka, KE-31.5510. Aalto-yliopiston teknillinen korkeakoulu, Kemian laitos. Kurssimateriaali. 2010. 86 p.
5. Kawai, Y and Shiraishi, Y. Hand book of Physico-chemical Properties at High Temperature. The Iron and Steel Institute of Japan, Special Issue (ISIJ) No. 41. 1988. 255 p.
6. Brillo, J., Egry, I. & Matsushita, T. Density and Surface Tension of Liquid Ternary Ni–Cu–Fe Alloys. International Journal of Thermophysics, Vol. 27, No. 6. 2006. pp. 1778-1791.
7. Egry, I., Brillo, J. & Matsushita, T. Thermophysical Properties of Liquid Cu-Fe-Ni alloys. Materials Science and Engineering A 413–414. 2005. pp. 460 - 464.
8. Smyth, J. Descriptive Mineralogy Sulfides. 2009 (online accessed 2010). URL address: http://ruby.colorado.edu/~smyth/G3010/15Sulfides.pdf
9. Wills, B.A. and Napier-Munn, T.J. Wills' Mineral Processing Technology, An Introduction to the Practical Aspects of Ore Treatment And Mineral Recovery. 7th edition. 2006. 444 p.
10. Roine, A. HSC Chemistry 7. Outotec Research Oy. 2010.
11. Makovicky, Emil & Brian, J. Skinner. Studies of the Sulfosalts of Copper. VI. Low-Temperature Exsolution in Synthetic Tetrahedrite Solid Solution, Cu12+xSb4+yS13. Canadian Mineralogist. 1978. Vol. 16. pp. 611-623.
12. Tatsuka, K. and Morimoto, N. Tetrahedrite Stability Relations in the Cu-Fe-Sb-S System. American Mineralogist. Vo. 62. 1977. pp. 1101-1109.
13. Tatsuka, Kiyoaki & Morimoto, Nobuo. Composition Variation and Polymorphism of Tetrahedrite in the Cu-Sb-S System below 400°C. American Mineralogist. Vol. 58. 1973. pp. 425-434.
14. Tenailleau, C., Etschmann, B., Wang, H., A. Pring, Grguric, B. A. and Studer, A.Thermal expansion of troilite and pyrrhotite determined by *in situ* cooling (873 to 373 K) neutron powder diffraction measurements (Abstract). Mineralogical Magazine, v. 69, no. 2. 2005. pp. 205-216.
15. Rajamani, V. and Prewitt, C.T. Thermal Expansion of the Pentlandite Structure. American Mineralogist, Volume 60. 1975. pp. 39 - 48.

16. Selivanov, E. N., Gulyaeva, R. I. and Vershinin, A. D. Thermal Expansion and Phase Transformations of Copper Sulfides. ISSN 0020-1685, Inorganic Materials. Vol. 43, No. 6. 2007. pp. 573 – 578.

17. Tatsuka, K. and Morimoto, N. Tetrahedrite Stability Relations in the Cu-Fe-Sb-S System. American Mineralogist. Vo. 62. 1977. pp. 1101-1109.

18. Friese, Karen, Grzechnik, Andrzej, Makovicky, Emil, Balic-Z unic, Tonc˘I & Karup-Møller, Sven. Crystal Structures of Iron Bearing Tetrahedrite and Tennantite at 25 and 250^{o}C by Means of Rietveld Refinement of Synchrotron Data. Phys Chem Minerals. 2008. pp. 455–465.

19. Zushu Li, Kenneth C. Mills, Malcolm McLean & Kusuhiro Mukai. Measurement of the Density and Surface Tension of Ni-Based Superalloys in the Liquid and Mushy States. Metallurgical and Materials Transactions B. Volume 36B. 2005. pp. 247-269.

20. Victor, Kress, Lori, E. Greene, Matthew, D. Ortiz, Luke Mioduszewski. Thermochemistry of Sulfide Liquids IV: Density Measurements and the Thermodynamics of O–S–Fe–Ni-Cu Liquids at low to Moderate Pressures. 2008. Contrib Mineral Petrol 156. 2008. pp. 785 – 797.

21. Nagamori, M. Density of Molten Ag-S, Cu-S, Fe-S, and Ni-S Systems. 1968. Transactions of the Metallurgical Society of AlME. Vol. 245. pp. 1897- 1902.

22. Nishida, K., Terasaki, H., Ohtani, E. and Suzuki, A.The effect of Sulfur Content on Density of the Liquid Fe–S at High Pressure. Phys Chem Minerals. 2008. pp. 417–423.

23. Miettinen, J. & Kytönen, H. Calculatin of Density in liquid Steels.Helsinki University of Technology Publications in Materials Science and Engineering. TKK-MT-187. 2006. 41 p.

24. Davenport, W.G., King, M., Schlesinger, M. and Biswas, A.K. Extractive Metallurgy of Copper. 4th edition. Elsevier Science Ltd. 2002. 412 p.

25. Davenport, W.G. and Partelpoeg, E. H. Flash Smelting, Analysis, control and Optimization. 2nd edition. Pergamon Press.1987. 324 P.

26. Toguri, J.M. and Ip, S.W. Surface and Interfacial Tension of the Ni-Fe-S, Ni-Cu-S, and Fayalite Slag Systems. Metallurgical Transactions B, Vol. 24B. 1993. pp. 657 – 668.

Appendix A

Experimental data for densities and coefficients A and B (in equation (10)) of the binary alloys in the Co-Cu-Ni-Fe system [5].

Co - Ni alloy				**Co - Cu alloy**			
at. % Ni	A	B	T(K)	at. % Co	A	B	T(K)
0	9.71	1.1	1793-1903	0	8.75	0.65	1500-1898
20	9.29	0.8	1798-1928	20	8.35	0.47	1653-1873
40	8.35	0.3	1798-1938	40	8.87	0.77	1698-1903
60	7.82	0.0	1783-1938	60	8.67	0.61	1703-1898
80	9.11	0.7	1788-1948	80	8.56	0.53	1748-1913
100	10.10	1.2	1763-1933	100	9.71	1.11	1793-1898
Co - Fe alloy				**Cu - Fe alloy**			
at. % Co	A	B	T(K)	at. % Fe	A	B	T(K)
0	8.78	0.9	1828-1938	0	8.75	0.65	1500-1898
20	9.28	1.1	1798-1913	20	8.90	0.84	1708-1898
40	9.44	1.1	1798-1913	40	9.20	1.10	1728-1918
60	9.58	1.1	1783-1903	60	7.88	0.43	1768-1923
80	9.56	1.0	1788-1918	80	8.81	1.01	1778- 1923
100	9.71	1.1	1793-1903	100	8.78	0.95	1833-1938
Cu - Ni alloy				**Fe - Ni alloy**			
at. % Ni	A	B	T(K)	at. % Ni	A	B	T(K)
0	8.75	0.6	1500-1898	0	8.78	0.95	1828-1938
20	8.36	0.4	1638 – 1873	20	9.08	1.03	1798-1923
40	8.12	0.2	1643-1888	40	8.73	0.80	1803-1913
60	8.00	0.2	1678-1918	60	7.57	0.10	1748-1923
80	8.32	0.3	1793-1918	80	9.38	0.93	1778-1918
100	10.10	1.2	1773-1928	100	10.1	1.27	1763-1933

Appendix B

Densities of phases in the Ni-Fe-S system at 1200^{o}C [26]. Compositions are in Wt. % and values in brackets are analyzed.

Ni	Fe	S	ρ(g/cm^3)
73.7	0.6	25.69	5.18
61.93	9.87	28.2	5.03
22.93	44.67	32.4	4.35
0	66.73	33.27	3.82
74.45	0.33	25.22	5.18
56.34	14.62	29.04	4.95
34.95	35.92	29.13	4.58
32.3	37.61	30.09	4.53
10.99	56.87	32.14	4.08
72.82	0	27.18	5.18
61.14	9.04	29.82	5.02
34.53	34.93	30.54	4.58
13.48	53.61	32.91	4.14
0	65.36	34.64	3.82
51.45	19.34	29.21	4.87
23.75	44.59	31.66	4.36
11.44	56.72	31.84	4.09

Densities of phases in the Ni-Cu-S system at 1200 ^{o}C [26]. Compositions are in Wt. % and values in brackets are analyzed.

Ni	Cu	S	ρ(g/cm^3)
63.80 (64.90)	15.76 (16.02)	18.80 (19.10)	5.18
38.83 (39.10)	40.70 (41.00)	19.70 (19.90)	5.22
59.20(59.30)	15.37 (15.40)	25.20 (25.30)	5.19
38.70 (39.57)	39.70 (40.59)	19.40 (19.83)	5.22
15.00 (15.46)	65.60 (67.63)	16.40 (16.91)	5.25
37.90 (38.70)	40.80 (41.68)	19.20 (19.61)	5.22
58.40 (59.17)	15.60 (15.80)	24.70 (25.02)	5.19
0.00 (0.00)	77.30 (78.80)	20.80 (21.20)	5.25

HELSINKI UNIVERSITY OF TECHNOLOGY PUBLICATIONS IN MATERIALS SCIENCE AND ENGINEERING

TKK-MT-201 Heikinheimo,E.,Selin,L.,(ed.),
Possibilities of electron excited microbeam analysis in materials science. Graduated School Seminar, 2008 at TKK, Espoo, Finland

TKK-MT-202 Miettinen, J.,
Tentative thermodynamic description of ternary Fe-Mo-B, Fe-Nb-B, Fe-Ti-B and Fe-V-B systems. 2008

TKK-MT-203 Kekkonen, M. (ed.),
Materials production and synthesis / 2008

TKK-MT-204 Heikinheimo, E., Selin, L. (editors),
Defect Structure and Reactivity of Solids. 2009

TKK-MT-205 Miettinen, J.,
Thermodynamic description of the Fe-Nb-Ti-V-C-N system. 2009

TKK-MT-206 Miettinen, J., Kytönen, H.,
Thermodynamic descriptions of Fe-Mn-Si, Fe-Mn-B and Fe-Si-B systems. 2009

TKK-MT-207 Huitu, K., Kekkonen, M., Holappa, L.,
Novel Steelmaking Processes. 2009

TKK-MT-208 Bunjaku, A., Holappa, L.,
Thermodynamic properties of NICKEL laterite ores. 2009

TKK-MT-209 Heikinheimo, E., Selin, L. (editors),
Quantitative electron probe microanalysis in materials science.
Graduate School Seminar, September 25, 2009 at TKK, Espoo, Finland

TKK-MT-210 Keski-Honkola A., Vaajoki, A., Oksanen, J., Hämäläinen, M.,
Ag-Bi-Cu-Sn seoksen termodynaaminen mallintaminen FactSage-ohjelmalla. 2009

TKK-MT-211 Kekkonen, M., (ed.),
Materials Production and Synthesis / 2009 MT-0.3201

TKK-MT-212 Isomäki, I., Hämäläinen, M., Pirso, J., Ferreira, J., Braga, H.
Thermodynamic and Structural Study of Quaternary Ni-rich Fe-Ni-Ti-W Phase Diagram. 2009

TKK-MT-213 Heikinheimo, E., (ed.),
Activity Report 2007 – 2009. Department of Materials Science and Engineering. 2010

TKK-MT-214 Tesfaye Firdu, F., Taskinen, P.,
Sulfide Mineralogy – Literature Review. 2010

ISBN 978 952-60-3272-6
ISSN 1455-2329